

A STUDY ON OPTICAL PROPERTIES OF SnS NANOPARTICLES

Ram Sharan, Research Scholar, Dept. of Physics, Swami Vivekanand University Sagar, MP
Dr. Anil Tiwari, Professor, Dept. of Physics, Swami Vivekanand University Sagar, MP

ABSTRACT

Nanoparticles are key components of Nanotechnology, serving as raw materials for the construction of Nanostructures, Nanomaterials, Nanomachines, and Nanodevices. Nanoparticles are defined as "particles with diameters of 100nm or less." Novel features that distinguish nanoparticles from bulk materials often emerge at a crucial length scale of less than 100 nm. SnS Nanotubules particles were synthesised by the solvothermal method using a precursor materials of tin and sulfur as $\text{SnCl}_2 \cdot 2\text{H}_2\text{O}$ and $\text{SC}(\text{NH}_2)_2$. The optical properties of the SnS was characterized by ultraviolet–visible (UV–Vis) analysis and fluorescence study. From the studies, the optical absorption of SnS nanoparticle, has the values of band gap energy (E_g) of 1.77 eV and from PL study the emission is absorbed.

KEYWORDS: optical properties, SnS nanoparticles, UV-Vis analysis, FTIR, XRD

INTRODUCTION

The study of phenomena & the manipulation of materials at atomic, molecular, & macromolecular sizes is known as nanoscience. Their physical and chemical properties are displayed at atomic/molecular levels with diameters ranging from a few nanometers to less than 100 nm, since attributes at this size differ dramatically from those at a larger or bulk scale.

Today, nanotechnology is a popular rising field of science and technology. It has grabbed the interest of experts from various disciplines, including physics, chemistry, biology, and engineering. In today's scientific world, the term nano refers to physical length scales on the order of a billionth of a metre. As a result, nano-scale materials exist in a physical size regime between bulk, macroscale materials (condensed matter physics) and molecule compounds (The realm of traditional chemistry). The emphasis on crystal structure is due to the fact that nanoscience and nanotechnology are concerned with nanometer-sized crystalline substances. [1].

Furthermore, the structural section depicts the rise in surface to volume ratio for nano-materials over bulk. This is due to the fact that in nanometer-sized systems, up to 50% of the atoms reside at the surface of a nanostructure, as opposed to macroscopic solids, where such quantities are normally significantly lower. When a substance is nanoscale in size, the surface might possibly influence its optical and electrical characteristics. Furthermore, the increase in surface area is significant in applications where the surface to volume ratio is vital, such as catalysis and photovoltaics. [2]

Energy scarcity & environmental pollution are two important difficulties for modern society's sustainable growth, necessitating novel materials research and the enhancement of their energy-storage and environmental qualities. Tin disulfide, one of the most significant metal-sulfide compounds, has a layered CdI_2 -type structure made of a tin cation sandwiched between two layers of sulphur anions comprises layers of Sn and S atoms securely bonded together with weak van der Waals interaction between layers. [3,4,5].

Most of the research in field of optoelectron solar cells based on sensitized CdS, CdSe, CdTe, PbS, PbSe, PbTe which are all of high toxic It also possesses favorable properties of semiconductor hetrostructure materials with respect to cost, availability, less toxicity & stability [6].

Semiconductors SnS, SnSe, GeS, and GeSe are expected to exhibit good chemical and environmental stability and show promise as low-cost solar cell components. Furthermore, they contain more environmentally friendly elements than alternative narrow-band-gap systems containing SnS, which are orthorhombic with a distorted rock-salt structure, have both indirect and direct band gaps that are closely spaced in energy, and are orthorhombic with a distorted rock-salt structure. Several research on the synthesis of SnS with typical SnS morphologies have been published: nanoplate-on-sheet and nanoparticle-on-sheet [7-10].

This chapter showed that morphology & size of particles as an active material with a method change of solvothermal [11]. In these present work in the solvothermal decomposition of preformed single source precursor thiourea in a mixture of co-ordinating with the solvent of ethyl alcohol at relatively in the low temperatures. This specific solvothermal approach has a strong potential for producing high grade SnS nanoparticles with predefined functions. The SnS nanoparticles generated using a novel solvothermal process exhibit significant optical absorption in the visible and near-infrared spectrum bands, making them ideal for spectroscopic behaviour alterations and inclusion into optical devices.

OBJECTIVES OF THE STUDY

- To investigate Optical Properties of SnS Nano Particles by Solvothermal Method

REVIEW OF RELATED LITERATURE

A. Tanusevski investigates the optical and photoelectric characteristics of SnS thin films grown through chemical bath deposition. Chemical bath deposition was used to generate thin films of SnS, which were then thermally treated in an argon environment at various temperatures. The films were polycrystalline with an orthorhombic structure when they were formed, but their preferred orientation increased after a 300 °C heat treatment. The transmittance spectrum determines the optical bandgap and kind of transition. Thermal treatment has no influence on the optical bandgap observed for direct transitions, which is 1.38 eV. The optical bandgap for indirect transitions increased with heat treatment time, and the phonon energy was determined. The red edge of photoconductivity spectrum also revealed a bandgap of $E_g(\text{ph}) = 1.24$ eV. The temperature development of films' dark resistance reveals an impurity level with an activation energy of 0.39 eV & a thermal bandgap of $E_g(\text{T}) = 1.19$ eV. [12]

Sulaeman, Yin, and Sato examine the solvothermal synthesis of tailored nonstoichiometric strontium titanate for efficient visible-light photocatalysis. Microwave-assisted solvothermal reactions of SrCl_2 and $\text{Ti}(\text{OC}_3\text{H}_7)_4$ in KOH aqueous solutions produced SrTiO_3 particles with varying Sr/Ti atomic ratios. SrTiO_3 nanoparticles of the perovskite type with particle diameters of 30-40 nm were produced. Photocatalytic activity was measured with light emitting diode lamps of various wavelengths, including 627 nm (red), 530 nm (green), 445 nm (blue), and 390 nm (UV). The photocatalytic activity was observed to vary greatly based on the Sr/Ti atomic ratio, with strontium rich sample (Sr/Ti atomic ratio > 1) exhibiting robust visible light responsive photocatalytic activity for NO oxidation. [13]

SnS nanocrystals were manufactured in a simple and easy way by Ning et al. Tin sulphide, which is used as a tin precursor, is made from $\text{Sn}_6\text{O}_4(\text{OH})_4$. By adjusting the reaction conditions, SnS nanocrystals of various shapes and sizes may be produced. SnS nanoparticles & nanoflowers with orthorhombic crystal structure have a consistent size distribution. SnS nanoflowers first transform into polycrystalline nanoflowers, then into amorphous nanosheets. The driving force of amorphization reduces high free energy of nanocrystals. The major reason of shape development and amorphization in SnS is its layered crystal structure. To investigate optical properties of nanoparticles, optical absorption spectra are utilised. The optical direct band gaps of SnS nanoparticles are 3.6 eV while the optical indirect band gaps are 1.6 eV. Both direct & indirect transitions in nanoparticles display a noticeable quantum-size influence when compared to the direct band gap (1.3 eV) & indirect band gap (1.09 eV) in bulk SnS. [14]

Wen Cai and colleagues used a biomolecule-assisted mild solvothermal technique using L-cysteine as sulphur source and complexing agent to effectively synthesise SnS microflowers with nanoplates. The as-prepared product's phase structure, morphology, composition, & optical characteristics were investigated using XRD, FE-SEM, TEM (HRTEM), SAED, XPS, TGA, and UV-vis spectrum. The as-synthesized product, according to findings, is made up of microflowers and nanoplates with an average thickness of 50 nm. A method for producing SnS microflowers using nanoplates was also presented & briefly discussed. The suggested solvothermal approach, which employs L-cysteine as a sulphur source and complexing agent, has great promise for low-cost and large-scale synthesis of a diverse spectrum of tin chalcogenide compounds. [15]

The current state of chalcopyrite thin film solar cell fabrication methods employing low-cost solution techniques was presented by Lee D. and Yong K. The development phases are compared in an evaluation of recently published articles providing liquid-based deposition methods. Finally, there is a debate & forecast. Thin-film solar cells containing chalcopyrite $\text{Cu}(\text{In}_{1-x}\text{Ga}_x)(\text{Se}_{1-y}\text{S}_y)_2$ absorbers (CIGSSe) have lately piqued the interest of researchers working to develop sustainable technologies for capturing clean energy. By substituting vacuum-based deposition processes with large-scale, high-throughput operations, nonvacuum solution approaches can lower manufacturing costs. Material efficiency can aid in the reduction of production costs. Non-vacuum procedures are often divided into two steps: solution coating and post-annealing. Non-vacuum procedures are classified as nanoparticle (NP) approaches or molecular precursor techniques based on when the CIGS phase arises. [16]

M.S. Selim and colleagues investigate the influence of film thickness on the structure and optical characteristics of a thermally evaporated SnS film. At normal temperature, SnS films with thicknesses ranging from 152 to 585nm were deposited on clean glass substrates. An X-ray diffraction study revealed that SnS films with a thickness of 283nm are crystalline, whereas films with a lower thickness are amorphous with a more crystalline background. A transmission electron microscope and the associated electron diffraction pattern were used to validate the crystalline nature of the bottom layer thickness. The chemical composition of the larger film samples was almost stoichiometric, but the thinner samples were low in S and high in Sn. In the wavelength range 350-2500nm, the optical properties of the deposited films were examined. As layer thickness rises, so does the refractive index. The refractive index for the film thicknesses tested is properly described by the effective-single-oscillator model. The static refractive index and dielectric constant have been computed. The optical absorption coefficient research showed the occurrence of a straight optical transition, with the matching band gap values dropping as the film thickness increased. [17]

Imen Bouhaf Kherchachi et al. study the impact of deposition time on structural, optical, and electrical properties of ultrasonic-sprayed Sn_xS_y films. At 300°C for $t=2\text{min}-10\text{min}$, Sn_xS_y thin films are produced on glass substrates using two precursors: tin (II) chloride & tin (IV) chloride, respectively. X-ray diffraction (XRD), UV-VIS-NIR optical transmittance tests, & four-point electrical resistivity measurements were used to analyse the films. The analysis of Sn_xS_y films using X-ray diffraction (XRD) revealed three crystallite phases: SnS_2 , SnS, and Sn_2S_3 . Furthermore, our results reveal that SnS_2 phase stability outperforms SnS and Sn_2S_3 phase stability. The visible spectrum findings of (UV) spectroscopy reveal that films created at 10min have low transmittance in the visible region for two precursors, and that a direct band gap decreases with increasing deposition time. Electrical studies show that the resistivity behaviour is influenced by the precursors utilised and the deposition duration. [18]

Srinivasa and Santhosh examine the effect of thickness on thin film structural, morphological, optical, and electrical characteristics. The development of single phase SnS films is supported by X-ray diffraction (XRD) and micro-Raman investigations. At a substrate temperature of 300°C , SnS thin films of various thicknesses were grown on glass substrates. SEM and atomic force microscopy were used to investigate changes in surface morphology, roughness, and average grain size of as-deposited films (AFM). Measurements of optical transmittance are used to determine optical characteristics of deposited thin films such as film thickness (d), absorption coefficient (a), optical band gap (E_g), refractive index (n), and extinction coefficient (k). The optical energy band gap shrinks as layer thickness increases, from 1.51 eV to 1.24 eV. From 170 nm to 915 nm, the electrical conductivity and photoconductivity of the films rise by more than two orders of magnitude. The apparent photoresponsivity and specific detectivity of the film increase as its thickness increases. The p-type character of the as-prepared SnS thin films is indicated by Hall effect measurements. [19]

SYNTHESIS OF SnS NANOROD

All reagents were used without further purification. Stannous chloride ($\text{SnCl}_2 \cdot 2\text{H}_2\text{O}$), thiourea NH_2CSNH_2 & ethyl alcohol other chemicals were of analytic grade &

purchased from Sigma-Aldrich. Synthesis of SnS Nanotubules particles similarly done by [20] 5mmol of SnCl₂ · 2H₂O and 7mmol of thiourea were dispersed in 50ml of ethyl alcohol then stirred for 1hour, after one hour a transparent solution obtained, now the stirred solution is transferred to the cylindrical 200ml capacity Teflon-lined stainless steel autoclave & maintained 180°C for 12hours, after the solvothermal treatment the sample with brown in color which is collected and subjected to washing procedure with di-ionized water & ethanol. The final obtained product was dried at 80°C. Obtained nanoparticles of ash color.

CHARACTERIZATION

The SnS nanoparticles were investigated by Optical absorbance characterization were recorded using a JASCO UV-Vis spectrophotometer in range of 300–800 nm, Panalytical X'PERT PRO Diffractometer with Cu-Kα monochromatic radiation source (λ = 1.5406 Å) in range of 2θ = 10–80 degree, Molecular vibrations of SnS Nanoparticles were carried out using a Perkin Elmer Fourier Transform Infrared (FTIR) Spectrometer (Model RX-I) with a wavelength range of 4000–400 cm⁻¹ using the KBr pellet method. Scanning Electron Microscopy (SEM, JSM-6700F) with an Energy-Dispersive X-ray Spectrometer (EDS).

RESULTS AND DISCUSSION

OPTICAL STUDIES OF UV-VIS-NIR ABSORPTION

UV-vis-NIR absorption spectra of SnS nanoparticles produced by solvothermal technique were measured in the 200–800 nm spectral region. The absorbance of SnS nanoparticles in the visible area (below 800nm) was reported to be high [21]. We calculated the optical band gap using the following equation:

$$(ah\nu)^n = (h\nu - E_g)^n \quad (1)$$

From this equation [22], direct band gap (E_{dir}) & indirect band gap (E_{indir}) can be obtained from n = 2 & n = 1/2, respectively. The insert plot in Fig 1 shows curves of (αhν)² versus hν on SnS for each temperature.

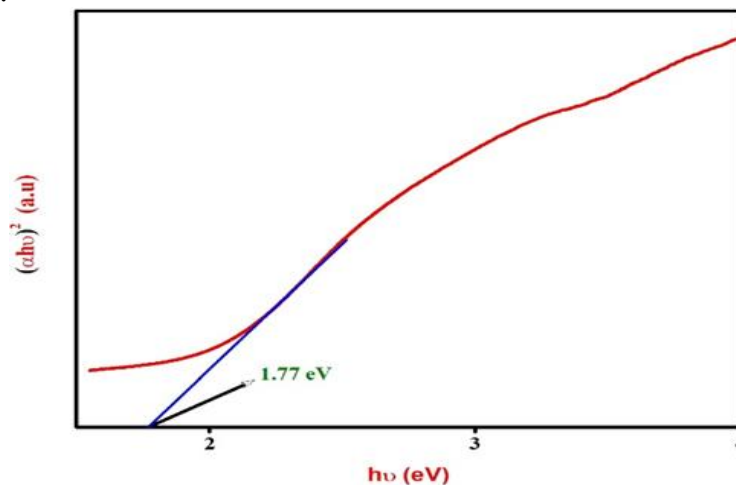


Fig: 1 Taucplot of SnS Nanotubules Particles

The optical band (E_{dir}) was calculated by taking the intercept of the linear extrapolation with photon energy at absorption start of the (hν)² curve. The optical absorption of SnS nanoparticles yielded band gap energy (E_g) values of 1.77 eV via direct band gap (related band gap value is published by Lewis et al [23]).

PHOTOLUMINESCENCE (PL) ANALYSIS

To understand optical behavior of SnS nanotubules particles PL measurements were carried out at room temperature. The emission peak is due to radiative recombination of quantum confined electron-hole pair whose energy is comparable to energy band gap of nanoparticles [24]. The recorded PL spectra demonstrate that the SnS nanoparticles show a sharp peak at the wavelength of 645 nm shown in Fig 2.

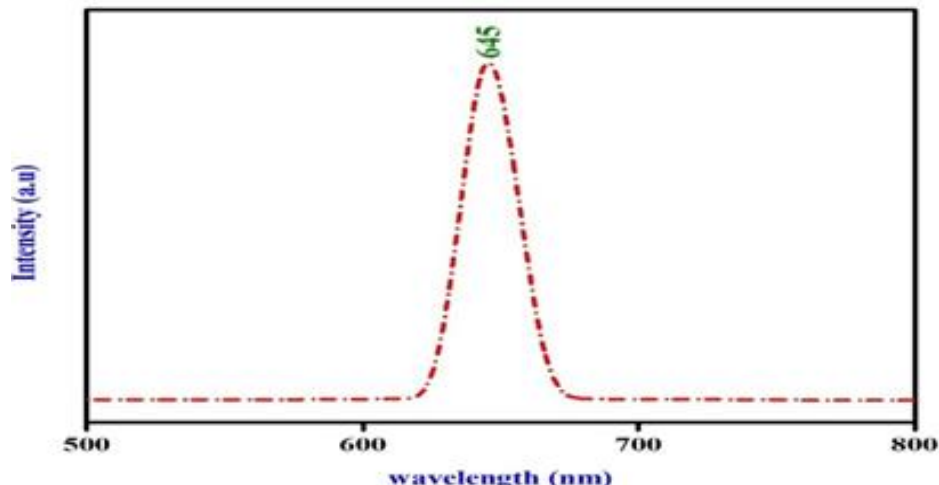


Fig 2 PL Spectrum of SnS Nanotubules Particles

The peak is of red emission probably originated from free carrier excitonic band edge transition b/w valence & conduction band at energy point of ~ 1.77eV, obtained results are matched [25]. No extra emission peak was observed, corroborating the absence of any other impurities, defects and trap centers in sample, thus confirming synthesized nanoparticles to be of pure SnS.

POWDER- XRD DIFFRACTION

The structural properties of SnS nanoparticles at different processing condition using X-Ray Diffractometer. The spectrum shown in Fig 3 promising net peaks at $2\theta = 25.96^\circ, 32^\circ, 38.30^\circ, 50.24^\circ, 65.32^\circ$ corresponding respectively to planes 120, 031, 140, 151 and 300 for orthorhombic crystal structure (JCPDS card data number 33 – 1375).

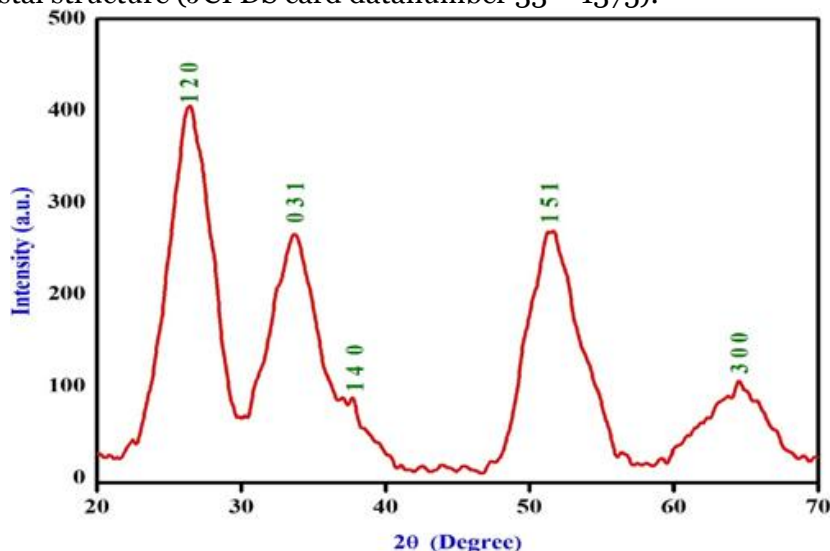


Fig 3 X-Ray Diffraction spectrum of SnS Nanotubules Particles

This result supports XRD results which show that sample contains pure phase of SnS. The crystalline structure of SnS particles can be indexed to that of the a-SnS, Herzenbergite modification (JCPDS 39-354) which is orthorhombic $a) 4.305\text{Å}, b) 11.262\text{Å}, c) 3.976\text{Å}$ [26]. the (120) peak intensities of SnS particles, The peak at 50.05° also be due to phase, as this corresponds to (151) reflection reported by David Avellaneda et al., [27] in also for SnS particles at 180°C were significantly higher intensity average grain size calculated from XRD results by the Scherrer formula,

$$D = \frac{0.9\lambda}{\beta \cos\theta} \dots\dots\dots (2)$$

Where, D denotes average grain size of crystal, 0.9 is constant related to crystalline shape (Scherrer constant), λ is wavelength of $\text{Cu K}\alpha$, β is full width at half maximum (FWHM) value, & θB is the Bragg angle where peak appears, average grain size was less than of 26 nm [28].

FTIR ANALYSIS

Fourier Transform Infrared Spectroscopy examination of as prepared SnS nanotubules particles. As revealed in Fig 4 the peaks at 1630 cm^{-1} pure SnS₂ are assigned to hydroxyl groups stretching vibration of hydrated oxide.

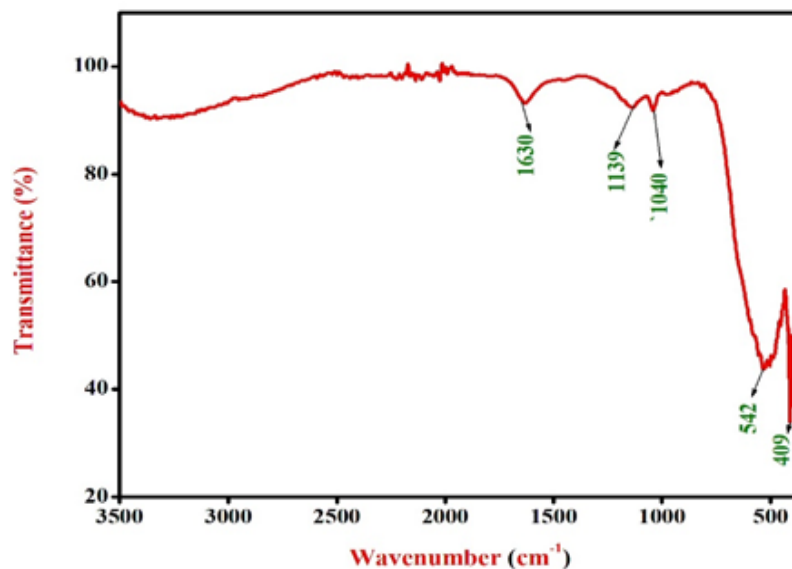


Fig 4 Fourier Transform Infrared spectrum of SnS Nanotubules Particles

The SnS bond spectra are present in between 1000 cm^{-1} – 1200 cm^{-1} [29]. In this prepared sample 1139 cm^{-1} and 1040 cm^{-1} indicate the SnS spectra in the above mentioned. Furthermore peak emerging at 542 cm^{-1} and 408 cm^{-1} is contributed by Sn-S vibration [30] Meanwhile, featured vibration of Sn-S bond in the prepared nanoparticles is invisible which is attributed to low content of SnS. Band observed between 1100 cm^{-1} and 1200 cm^{-1} for all samples are attributed to presence of inorganic compound of them reveal presence of thioure group similarly reported [31].

CONCLUSIONS

Nanotechnology is a relatively new and promising discipline due to the unique and practical uses of nanomaterials (NM), which serve as the foundation for many technical and scientific sectors. Because of the discovery of exciting and unique features of matter at the nanoscale, this discipline has opened the door to the development of an infinite number of novel materials. The extent of the range of scientific and technical applications based on nano-based concepts explains and justifies the impact of nanotechnology on current civilization. It is obvious that these items will end up in the environment sooner or later. Although engineered nanoparticles are designed to serve a specific purpose, and we may have an idea of their original properties during production, the fate and properties of the NPs once released into the environment may differ partially or completely from their original physicochemical properties for a variety of reasons: They may form macroscale aggregates, become covered with organic matter in the environment, or interact with other inorganic nanosized particles in nature, as described in the study.

SnS nanotubules particles are successfully synthesized by solvothermal method at 180°C. In UV-VIS absorption spectrum of a nanoparticles have a wide absorption range and 1.77 eV direct allowed transition energy gap, Powder XRD a strong peaks, which confirms the Herzenbergite orthorhombic crystal structure, by morphology study the rod shape appear. The Fourier transform infrared (FTIR) result also confirmed the SnS vibration at 1630 cm^{-1} , 1139 cm^{-1} , 1040 cm^{-1} , 542 cm^{-1} and 409 cm^{-1} . Based on these results shown that the SnS nanotubules were confirmed and optical studies reveal the materials promising for application in optoelectronics devices.

REFERENCES

1. Gleiter, H. (2000). Nanostructured materials: basic concepts and microstructure. *Acta materialia*, 48(1), 1-29.
2. Skorokhod, V. V., Uvarova, I. V., & Ragulya, A. V. (2001). Physico-chemical kinetics in nanostructured systems. *Kyiv: Academperiodica*, 1, 180-192.
3. Xiao, G., Wang, Y., Ning, J., Wei, Y., Liu, B., Yu, W. W., Zou, B. (2013). Recent advances in IV–VI semiconductor nanocrystals: synthesis, mechanism, and applications. *RSC Advances*, 3(22), 8104.
4. Yao, K., Li, J., Shan, S., & Jia, Q. (2017). One-step synthesis of urchinlike SnS/SnS₂ heterostructures with superior visible-light photocatalytic performance. *Catalysis Communications*, 101, 51–56.
5. Zai, J.; Qian, X.; Wang, K.; Yu, C.; Tao, L.; Xiao, Y.; Chen, J. Zai, J., Qian, X., Wang, K., Yu, C., Tao, L., Xiao, Y., & Chen, J. (2012). "3D-hierarchical SnS₂ micro/nano-structures: controlled synthesis, formation mechanism and lithium ion storage performances. *CrystEngComm*, 14(4), 1364–1375. "CrystEngComm 2012, 14, 1364–1375.
6. Mukaibo, H., Yoshizawa, A., Momma, T., & Osaka, T. (2003). Particle size and performance of SnS₂ anodes for rechargeable lithium batteries. *Journal of Power Sources*, 119-121, 60–63 *Chem. Commun.* 2011, 47, 1270–1272
7. Chang, K., Wang, Z., Huang, G., Li, H., Chen, W., & Lee, J. Y. (2012). Few-layer SnS₂/graphene hybrid with exceptional electrochemical performance as lithium-ion battery anode. *Journal of Power Sources*, 201, 259–266. doi:10.1016/j.jpowsour.2011.10.132
8. Xiao, G., Wang, Y., Ning, J., Wei, Y., Liu, B., Yu, W. W. ... Zou, B. (2013). Recent advances in IV–VI semiconductor nanocrystals: synthesis, mechanism, and applications. *RSC Advances*, 3(22), 8104.
9. Jiang, X., Yang, X., Zhu, Y., Shen, J., Fan, K., & Li, C. (2013). In situ assembly of graphene sheets-supported SnS₂ nanoplates into 3D macroporous aerogels for high-performance lithium ion batteries. *Journal of Power Sources*, 237, 178 186.
10. Luo, B., Fang, Y., Wang, B., Zhou, J., Song, H., & Zhi, L. (2012). Two dimensional graphene–SnS₂ hybrids with superior rate capability for lithium ion storage. *Energy Environ. Sci.*, 5(1), 5226–5230.
11. Devika, M., Reddy, N. K., Ramesh, K., Gunasekhar, K. R., Gopal, E. S. R., & Reddy, K. T. R. (2006). Influence of annealing on physical properties of evaporated SnS films. *Semiconductor Science and Technology*, 21(8), 1125–1131.
12. Tanusevski, A. (2003) Optical and photoelectric properties of SnS thin films prepared by chemical bath deposition. *Semiconductor Science and Technology*, Volume 18, Number 6, 501.
13. Sulaeman, U., Yin, S., & Sato, T. (2010). Solvothermal synthesis of designed nonstoichiometric strontium titanate for efficient visible-light photocatalysis. *Applied Physics Letters*, 97(10), 103102.
14. Ning et al. (2010). Facile synthesis of IV–VI SnS nanocrystals with shape and size control: nanoparticles, nanoflowers and amorphous nanosheets. *Nanoscale*, 2(9), 1699-1703.
15. Wen Cai et al. (2012) "Synthesis and characterization of nanoplate-based SnS microflowers via a simple solvothermal process with biomolecule assistance", *Advanced powder Technology* 23 (2012) 850-854.
16. Junfeng Chao et al. (2013) "Tin sulfide nanoribbons as high performance photoelectrochemical cells, flexible photodetectors and visible-light-driven photocatalysts", *RSC Advances Issue 8*, 2013.
17. M.S. Selim et al. (2013) "Effect of thickness on optical properties of thermally evaporated SnS films", *Thin Solid Films*, 2013, 527, 164-169, journal ISSN:0040-6090, DOI-10.1016/j.tsf.2012.10.019

18. Imen Bouhaf Kherchachi et al. (2016) "The synthesis, characterization and phase stability of tin sulfides (SnS₂, SnS and Sn₂S₃) films deposited by ultrasonic spray", September 2016 *Main Group Chemistry* 15(3):231-242, DOI:10.3233/MGC-160202
19. Srinivasa and Santhosh (2016) "Co-evaporated SnS thin films for visible light photodetector applications", October 2016, *RSC Advances* 6(98):95680, DOI:10.1039/c6ra20129f
20. Chauhan, H., Singh, M. K., Hashmi, S. A., & Deka, S. (2015). Synthesis of surfactant-free SnS nanorods by a solvothermal route with better electrochemical properties towards supercapacitor applications. *RSC Advances*, 5(22), 17228–17235.
21. Wang, Z., Qu, S., Zeng, X., Liu, J., Zhang, C., Tan, F. ... Wang, Z. (2009). The application of SnS nanoparticles to bulk heterojunction solar cells. *Journal of Alloys and Compounds*, 482(1-2), 203–207.
22. Tripathi, A. M., & Mitra, S. (2014). Tin sulfide (SnS) nanorods: structural, optical and lithium storage property study. *RSC Advances*, 4(20), 10358.
23. Lewis, D. J., Kevin, P., Bakr, O., Murny, C. A., Malik, M. A., & O'Brien, P. (2014). Routes to tin chalcogenide materials as thin films or nanoparticles: a potentially important class of semiconductor for sustainable solar energy conversion. *Inorg. Chem. Front.*, 1(8), 577–598.
24. Sunil H. Chaki*, M. P. Deshpande, Mahesh D. Chaudhary, and Kanchan S. Mahato (2013) "Synthesis and Characterization of Tin Monosulfide Nanoparticles" *Adv. Sci. Eng. Med.*, Vol. 5, No. 3.
25. M. Devika¹, N. Koteswara Reddy*,^{1,2}, M. Prashantha², K. Ramesh², S. Venkatramana Reddy³, Y. B. Hahn⁴, and K. R. Gunasekhar., (2010) "The physical properties of SnS films grown on lattice-matched and amorphous substrates", *Phys. Status Solidi A* 207, No. 8, 1864–1869
26. Stephen G. Hickey, Christian Waurisch, Bernd Rellinghaus, and Alexander Eychmüller* (2008) "Size and Shape Control of Colloidally Synthesized IV-VI Nanoparticulate Tin (II) Sulfide" *J. AM. CHEM. SOC.* 130, 14978–14980
27. David Avellaneda, M. T. S. Nair and P. K. Nair, (2008) "Polymorphic Tin Sulfide Thin Films of Zinc Blende and Orthorhombic Structures by Chemical Deposition" *J. Electrochem. Soc.*, Volume 155, Issue 7, Pages D517-D525.
28. Ham, G., Shin, S., Park, J., Choi, H., Kim, J., Lee, Y.-A. ... Jeon, H. (2013). Tuning the Electronic Structure of Tin Sulfides Grown by Atomic Layer Deposition. *ACS Applied Materials & Interfaces*, 5(18), 8889–8896.
29. Tarkas, H. S., Marathe, D. M., Mahajan, M. S., Muntaser, F., Patil, M. B., Tak, S. R., & Sali, J. V. (2017). Synthesis of tin monosulfide (SnS) nanoparticles using surfactant free microemulsion (SFME) with the single microemulsion scheme. *Materials Research Express*, 4(2), 025018.
30. Zhu, A., Qiao, L., Jia, Z., Tan, P., Liu, Y., Ma, Y., & Pan, J. (2017). C–S bond induced ultrafine SnS₂ dot/porous g-C₃N₄ sheet 0D/2D heterojunction: synthesis and photocatalytic mechanism investigation. *Dalton Transactions*, 46(48), 17032–17040.
31. Srivind, J., Balamurugan, S., Usharani, K., Prabha, D., Suganya, M., Nagarethinam, V. S., & Balu, A. R. (2018). Visible light irradiated photocatalytic and magnetic properties of Fe-doped SnS₂ nanopowders. *Journal of Materials Science: Materials in Electronics*, 29(11), 9016–9024.